Characterization of a TrkB-derived Phosphopeptide Inhibitor of PLCγ1

by

Chin Huat Tan

Department of Biochemistry
Duke University

Date:_____

Approved:

_____
Pei Zhou, Supervisor

_____
Margarethe Kuehn

_____
James McNamara

Thesis submitted in partial fulfillment of
the requirements for the degree of Master of Science in the Department of
Biochemistry in the Graduate School
of Duke University

2018

ABSTRACT

Characterization of a TrkB-derived Phosphopeptide Inhibitor of PLCγ1

by

Chin Huat Tan

Department of Biochemistry
Duke University

Date:_____

Approved:

_____
Pei Zhou, Supervisor

_____
Margarethe Kuehn

_____
James McNamara

An abstract of a thesis submitted in partial fulfillment of the requirements for the degree of Master of Science in the Department of Biochemistry in the Graduate School of Duke University

2018

Abstract

Epilepsy is a syndrome that affects about 65 million people around the world. About 150,000 new cases of epilepsy are reported in the United States every year. Temporal lobe epilepsy (TLE) is the most common form of human epilepsy. It is a chronic neurological disorder characterized by recurrent seizures that are devastating due to a lack of effective treatment. TLE is resistant to anticonvulsants and one-third of patients diagnosed with TLE are refractory to medication.

Excessive activation of tropomyosin receptor kinase B (TrkB) promotes TLE. The importance of phospholipase Cγ1 (PLCγ1) as a major downstream signaling effector of TrkB was first identified by the McNamara lab at Duke. Thus, selective inhibition of the PLCγ1-TrkB interaction constitutes a promising avenue for new drugs.

As a proof-of-concept, the McNamara lab engineered a novel 14-mer peptide pY816 that effectively inhibits epilepsy and prevents anxiety-like behavior induced by continuous seizure activity (status epilepticus), in a dose- and time-dependent manner. Despite their promising therapeutic effectiveness, the molecular details of the engagement of these inhibitors with PLCγ1 have remained elusive.

In this study, we propose x-ray crystallography and solution NMR studies to elucidate the binding mode of the peptide to PLCγ1 tandem SH2 domains. This will

ultimately facilitate the development of novel therapeutics targeting the TrkB-PLCγ1 interaction.

Contents

Abstract iv

List of Tables viii

List of Figures ix

List of Abbreviations x

1. Introduction 1

1.1 TrkB Signaling Pathway 1

1.1.1 PLCγ1 as The Dominant Downstream Effector in the TrkB Signaling 3

1.2 Architecture and Function of PLCγ1 Enzyme 4

1.3 The pY816 Peptide Targeting PLCγ1 6

2. Expression, purification, and characterization of the Src-homology 2 (SH2) domains of PLCγ1 in complex with the pY816 peptide 8

2.1 Expression and Purification of Human PLCγ1 SH2 domains 9

2.2 Determine the Affinity Constant of the pY816-PLCγ1 Tandem SH2 Domains Complex 10

2.3 NMR 2D ^{1}H-^{15}N HSQC Titration with the pY816 Peptide 12

2.4 Crystallization of the pY816-PLCγ1 Tandem SH2 Domains Complex 13

2.5 Alternative Approach: NMR 2D ^{1}H-^{15}N HSQC Titration of pY816 against individual SH2 domains 14

2.6. Methods and Materials 18

2.6.1 Optimization of PLCγ1 tandem SH2 domains purification 18

2.6.2 NMR titration experiments 19

2.6.3 Crystallization of the pY816-PLCγ1 tandem SH2 domains complex.....22

3. Conclusion 24

References 25

List of Table

Table 1: 2D ^{1}H-^{15}N HSQC titration experiment of pY816 peptide into PLCγ1 tandem SH2 domains 20

Table 2: 2D ^{1}H-^{15}N HSQC titration experiment of pY816 peptide into nSH2 or cSH2 domains.....21

List of Figures

Figure 1: The TrkB Signaling Pathway. 2

Figure 2: PLCγ1 Domain Architecture and the Structure of the Tandem SH2 domains.... 5

Figure 3: Selective Inhibition of PLCγ1 by pY816 7

Figure 4: SDS-PAGE Illustrating Purification of the Tandem SH2 Domains of PLCγ1 .. 10

Figure 5: SPR Sensorgram 11

Figure 6: Overlay NMR 2D ^{1}H-^{15}N HSQC Spectra of the ^{15}N labelled nSH2-cSH2 Domain Titrated with the pY816 Peptide 13

Figure 7: Initial Crystallization Hits 14

Figure 8: Overlay of NMR 2D ^{1}H-^{15}N HSQC Spectra of the ^{15}N-labelled nSH2 Domain (A) and cSH2 Domain (B) Titrated with Different Concentrations of the pY816 Peptide. 16

Figure 9: Plot of change in chemical shift of amide resonances versus molar ratio (pY816 concentration/final protein concentration)..... 17

List of Abbreviations

BDNF – Brain-Derived Neurotropic Factor
cSH2 – C-terminal SH2 Domain
DTT – Dithiothreitol
EEG – Electroencephalogram
HSQC – Heteronuclear Single Quantum Coherence
IP3 – Inositol 1,4,5-trisphosphate
IPTG – Isopropyl β-D-1-thiogalactopyranoside
ITC – Isothermal Titration Calorimetry
KA – Kainic acid
kDa – kiloDaltons
MALDI-TOF – Matrix-Assisted Laser Desorption/Ionization (MALDI)- Time of Flight (TOF)
mM – millimolar
MW – Molecular Weight
Ni-NTA – Nickel-Nitrilotriacetic Acid
NMR – Nuclear Magnetic Resonance
nSH2 – N-terminal SH2 Domain
PEG – Polyethylene Glycol
PIP2 – Phosphatidylinositol 4,5-bisphosphate
PLCγ1 – Phospholipase Cγ1
pTyr – Phosphorylated Tyrosine
RTK – Receptor Tyrosine Kinase
SDS-PAGE – Sodium dodecyl sulfate polyacrylamide gel electrophoresis
SE – Status Epilepticus
SENP1 – Sentrin-specific Protease 1
SPR – Surface Plasmon Resonance
SUMO – Small Ubiquitin-like Modifier
TLE – Temporal Lobe Epilepsy
TR-FRET – Time-resolved Fluorescence Resonance Energy Transfer
TrkB – Tropomyosin Receptor Kinase B
μM – micromolar

1. Introduction

The temporal lobe is one of the four major lobes in human brain, and it is associated with language comprehension, production of speech, sensory and emotion processing, as well as the formation of visual memory (*33*). Temporal lobe epilepsy (TLE) is a serious neurological disorder characterized by recurrent seizures, memory loss, and inability to respond to stimuli (*1*). TLE is the most common form of human epilepsy, and it accounts for nearly 30-40% of all cases associated with epilepsy. Prolonged seizures without proper and immediate treatment can result in death. Currently available drugs prescribed for TLE are non-specific and have limited clinical efficacy. About one-third of patients diagnosed with TLE are refractory to medication (*24*).

1.1 TrkB Signaling Pathway

Receptor tyrosine kinases (RTKs) have emerged as one of the key components in intracellular signaling cascades. Recent discoveries have shown that mutations in RTKs are causally linked to numerous diseases, such as cancer, diabetes, inflammation, and arteriosclerosis (*16*). RTKs have been extensively studied for decades. However, little is known about the mechanism of recruitment of their downstream effectors.

Humans have 58 known RTKs, which can be categorized into 20 subfamilies (*16*). All RTKs share a similar domain organization. A single transmembrane helix acts as a membrane anchor, and it is attached to a ligand binding domain in the extracellular region. It is also connected to a tyrosine kinase domain in the cytoplasmic region via a

juxtamembrane linker, and has a C-terminal tail for signal regulation, as shown in Figure 1 (*16*, *18*).

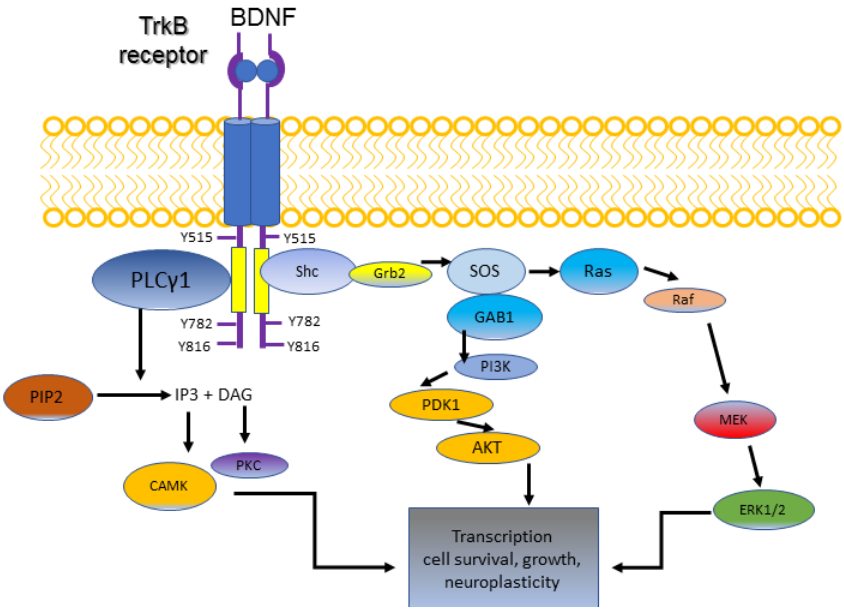

Figure 1: The TrkB signaling pathway. The autophosphorylation of TrkB triggers the binding of PLCγ1 and Shc proteins to activate various signaling cascades.

In general, the activation of RTKs is driven by dimerization upon binding to their cognate growth factor receptor (*18*). Each tyrosine kinase domain is *cis*-autoinhibited by its unique intramolecular interactions involving tyrosine residues (*16*). Following ligand-induced dimerization, this autoinhibition is released via autophosphorylation of these tyrosine residues, thereby creating docking sites for downstream effectors.

Tropomyosin receptor kinase B (TrkB) is a member of the human RTKs, and it is critical for neuronal survival, proliferation, and differentiation. TrkB has been causally linked to numerous neurological diseases, include Alzheimer disease, Huntington

disease, depression, addiction, and epilepsy (*17*). Neurotrophin brain-derived neurotrophic factor (BDNF) is a growth factor ligand that binds to TrkB to induce TrkB dimerization. TrkB dimerization triggers the phosphorylation of Tyr-515 and Tyr-816 in the intracellular domain, creating docking sites for PLCγ1 and Shc proteins, as shown in Figure 1 (*7*, *32*).

1.1.1 PLCγ1 as The Dominant Downstream Effector in the TrkB Signaling

The mechanisms underlying epileptogenesis are not well studied. The development of epileptogenesis may be due to abnormality in brain wiring, or imbalance in inhibitory and excitatory neurotransmitters (*23*). Patients with TLE often experience continuous seizure activity (status epilepticus [SE]) years before the onset of life-long TLE (*2*, *23*). The latent period (few months or years) between the initial occurrence of SE and the emergence of chronic TLE represents an opportunity for therapeutic interventions (*23*). Understanding the signaling pathway that promotes epileptogenesis is crucial, and it may provide novel insights for the development of therapeutic agents targeting TLE.

Experimental models have been developed to mimic the human seizure state. TLE can be induced by pharmacologic agents (kainic acid) or electrical stimulation, with the former being more commonly used to study epilepsy (*21*, *23*). The electroencephalogram (EEG) recording is used to monitor the electrical activity in the brain caused by seizures.

Previous studies have shown that transient inhibition of TrkB after status epilepticus prevents the occurrence of seizures, reduces anxiety-like behavior and the

destruction of hippocampal neurons (*4*). These studies demonstrate that the excessive activation of TrkB is required for the induction of TLE (*4, 10*). Recently, it was reported that PLCγ1, a binding partner of the TrkB receptor, serves as the dominant downstream signaling effector that promotes the development of TLE (*10*). Together, these findings establish uncoupling PLCγ1 from its TrkB receptor as an appealing strategy for drug development to prevent TLE.

1.2 Architecture and Function of PLCγ1 Enzyme

Mammalian phosphoinositide-specific phospholipase C (PLC) enzymes are divided into six families (β, γ, δ, ε, ζ, η), with 13 isoforms in humans (*13*). PLC enzymes share a conserved core architecture consisting of a pleckstrin homology (PH) domain, an EF-hand, a catalytic triosephosphate isomerase (TIM) barrel and a C-terminal C2 domain (Figure 2A). The catalytic TIM barrel domain is split into X- and Y-boxes by a X-Y linker. The N-terminal SH2 domain (nSH2), C-terminal SH2 domain (cSH2), and SH3 domain are inserted between the X- and Y-boxes of the TIM barrel catalytic domain (*13*).

The C2 and PH domains cooperate to direct PLCγ1 to the plasma membrane to perform its phospholipase activity. The PH domain also binds with inositides present in the plasma membrane, and it also acts as a membrane anchor (*12*). The catalytic TIM barrel is the most conserved domain, both structurally and functionally across all PLC isoforms. Both the nSH2 and cSH2 domains share about 35% sequence identity (*11*). The crystal structure of the nSH2-cSH2 domains was solved recently, and the structure reveals a

common SH2 domains architecture of two α-helices flanking antiparallel β-sheet (Figure 2B, PDB: 4EY0) [*26*].

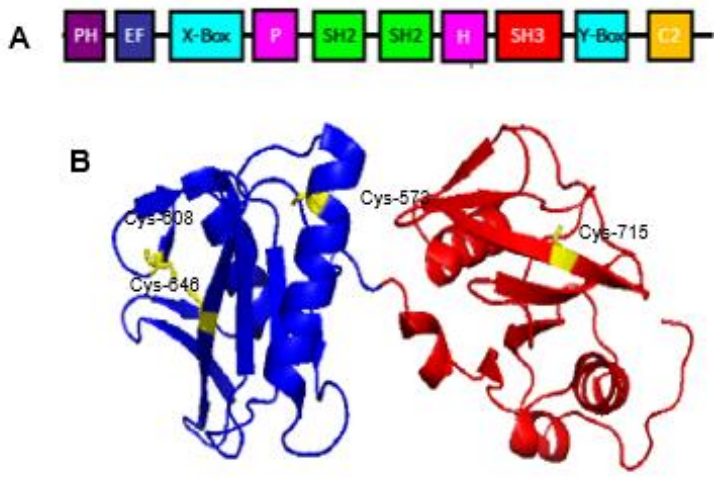

Figure 2: PLCγ1 domain architecture and the structure of the tandem SH2 domains (A). Architecture of PLCγ1 that consists of a N-terminal PH domain, an EF-hand, a catalytic TIM barrel comprised of X and Y boxes, and a C-terminal C2 domain. (B). Structure of the PLCγ1 tandem SH2 domains. The SH2 domains consist of antiparallel β-sheet sandwiched in between two α-helices. Blue indicates the nSH2 domain whereas red shows the cSH2 domain. Three cysteine residues in the nSH2 domain and one cysteine residue in the cSH2, as shown in yellow. (PDB:4EY0).

PLC enzymes are involved in a wide array of signaling mechanisms. They bind to different regulatory protein receptors, such as G protein subunits, receptor tyrosine kinases, and lipid components of the cellular membrane (*6*). It was previously reported that the phospholipase activity of PLC isoforms is basally inhibited by the cSH2 domain within the X-Y linker (*14, 15*). Tyrosine phosphorylation on the cSH2 domain, primarily on Tyr 783 induces a large conformational rearrangement and triggers the release of autoinhibition. Upon activation by its RTK, PLC catalyzes the hydrolysis of PIP2 in the

plasma membrane, to generate diacylglycerol as a second messenger and inositol 1,4,5-trisphosphate (IP3) [*13*]. IP_3 acts as a cofactor for the calmodulin kinase dependent pathway, and diacylglycerol serves as a second messenger in the protein kinase C pathway (*8*). These molecules are essential to regulate multiple cellular processes, including cell fertilization, proliferation, differentiation, and chemotaxis (*14*).

1.3 The pY816 Peptide Targeting PLCγ1

The excessive activation of TrkB has been causally implicated in TLE (*3,25,30*). The central role of phospholipase Cγ1 (PLCγ1) as the dominant downstream signaling effector that promotes the onset of TLE has been discovered by the McNamara lab. Thus, uncoupling of PLCγ1 from its receptor TrkB was demonstrated to be a novel avenue to prevent TLE (*10*).

This was accomplished using a novel 14-mer peptide pY816 (LQNLAKASPVpYLDI) that is engineered based on the phosphorylation site at the C-terminal region of the TrkB receptor that is required for the binding of PLCγ1. The peptide is fused with the TAT sequence to facilitate transfer across cell membranes

Extensive in vivo and genetic studies by the McNamara group have shown the binding specificity of the pY816 peptide to PLCγ1, and the ability of the peptide to cross the blood-brain barrier when administered intravenously, through mouse-model studies. Interestingly, the number of spontaneous recurrence seizures (SRS) decreased

significantly after pY816 injection as compared to the control (Figure 3) [*10*]. Reduced anxiety-like behavior was also demonstrated using a light-dark emergence test (*3*).

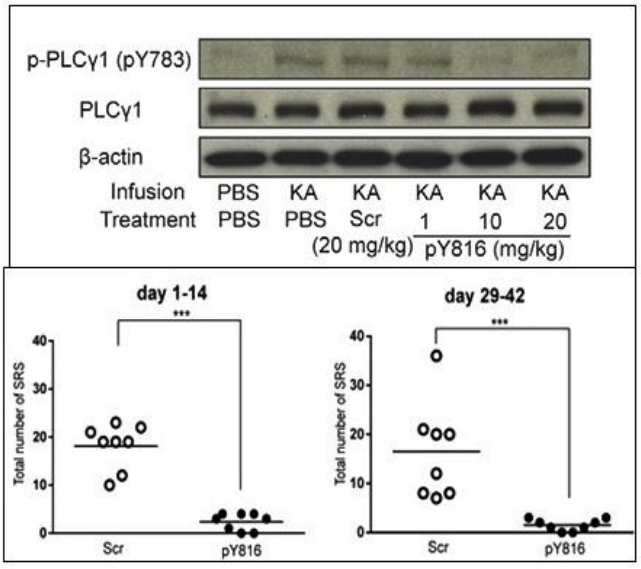

Figure 3: Selective inhibition of PLCγ1 by pY816. The top panel shows the decreasing in phosphorylation level of PLCγ1, with an increasing concentration of the pY816 peptide. Kainic acid (KA) is a chemoconvulsant. In this experiment, a scrambled peptide (Scr) was used as a control. The bottom panel shows the efficacy of the peptide in reducing the total number of seizures in mouse model studies (*10*).

In this proposal, we seek to utilize a combination of structural and biochemical studies to elucidate the molecular basis of the binding of the pY816 peptide to PLCγ1. The binding of the peptide to PLCγ1 causes disruption of the TrkB-PLCγ1 complex. This disruption of the TrkB-PLCγ1 complex reduces the phosphorylation of PLCγ1 mediated by TrkB, thus reducing the seizure numbers.

2. Expression, purification, and identification of the interacting Src-homology 2 (SH2) domains of PLCγ1 in complex with the pY816 peptide

The goal of this study is to investigate the binding mode of PLCγ1 tandem SH2 domains complexed with the pY816 peptide using X-ray crystallography. The engagement of PLCγ1 tandem SH2 domains with its RTK is under significant debate. Previous studies have revealed two conflicting binding modes of the PLCγ1 tandem SH2 domains when complexed with its RTK. We have developed an optimized protocol to obtain pure and homogenous samples of tandem nSH2-cSH2 domains of PLCγ1. To prepare samples for co-crystallization of the complex, we utilized SPR experiments to identify the affinity constant of the PLCγ1 tandem SH2 domains-pY816 complex. Random matrix screening was performed to determine the optimal conditions for crystal growth. The molecular properties at the binding interfaces will provide insights on the structural mechanisms that the pY816 peptide uses to bind to PLCγ1 tandem SH2 domains.

As an alternative, we propose to identify the SH2 domain that preferentially forms a complex with the pY816 peptide, utilizing 2D ^{1}H-^{15}N HSQC NMR spectroscopy. This shall aid in our crystallographic efforts. Preliminary NMR studies suggest that pY816 is likely to interact with the cSH2 domain of PLCγ1, as evident from the concentration dependent chemical shift perturbations as shown in Figure 8.

SH2 domains are small protein modules that mediate protein-protein interactions, such as autoinhibition, activation, and dimerization of their binding proteins. These small

protein modules are important for polypeptide and protein motifs recognition through phosphorylated tyrosines (pTyr) in the RTK (*4*, *15*). Previous reports have shown that an SH2 domain recognizes phosphotyrosine residues at the cytoplasmic region of its receptor, and the binding of PLCγ1 tandem SH2 domains to its receptor occurs in a sequence specific manner (*41*, *42*). This is critical for the specificity of the SH2 domains to bind to different pTyr-containing peptide ligands.

2.1 Expression and Purification of Human PLCγ1

We obtained expression constructs of human PLCγ1 containing the tandem SH2 domain from the McNamara lab at Duke. Unless otherwise noted, all the work described here with purified PLCγ1 contains only the nSH2 and cSH2 domains.

PLCγ1 tandem SH2 domains is a monomeric protein with molecular weight of 29kDa and it contains 246 amino acids (from 545 Histidine to 791 Proline). It contains 115 residues in nSH2 domain and 131 residues in cSH2 domain. There is 35% sequence identity between the nSH2 and cSH2 domains. (*11*).

PLCγ1 tandem SH2 domains was cloned into a SUMO-fusion expression vector in *E. coli*. The tandem SH2 domains construct contains a 10X Histidine tag and a SUMO tag at the N-terminus. SUMO is a ubiquitin-like protein that has been shown to improve protein solubility and expression. PLCγ1 tandem SH2 domains was expressed in the BL21(DE3) strain of *E. coli*. Cells were grown to OD_{600} of 0.5-0.8, and induced with IPTG overnight at 20°C. The protein was purified via nickel-affinity chromatography (Ni^{2+}-

NTA), and elution fractions were pooled, and purified to homogeneity using size exclusion chromatography, in buffer containing 10mM HEPES and 150mM NaCl (Figure 4). The SUMO tag was removed using a SUMO protease to prevent any potential interactions between the SUMO tag and the inhibitors that could add complications to our studies.

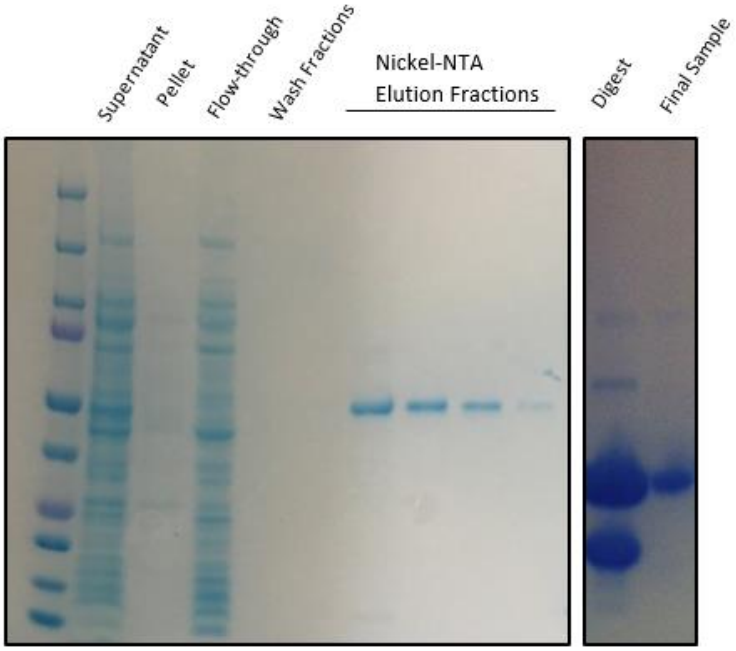

Figure 4: SDS-PAGE gel illustrating purification of the tandem SH2 domains of PLCγ1. The final lane is the highly pure and homogenous sample used in this study.

2.2 Determine the Affinity Constant of the pY816-PLCγ1 Tandem SH2 Domains Complex

To prepare sample for co-crystallization of the pY816-PLCγ1 tandem SH2 domains complex, we first need to determine the binding affinity of the complex.

Surface plasmon resonance (SPR) experiments are commonly used to detect protein-protein or protein-ligand interactions. SPR allows us to observe real-time binding, determine the on and off rates of the binding, and define affinity constants. The McNamara lab performed SPR experiments, and an initial affinity constant of the pY816-PLCγ1 tandem SH2 domains complex determined from SPR was 68.8 nM (Figure 5).

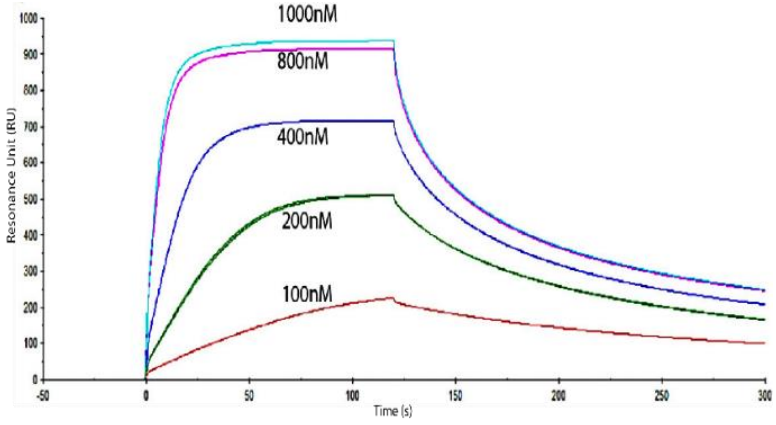

Figure 5. SPR sensorgram. The resonance units correspond to each concentration are plotted against time. The dissociation constant was determined from the ratio of k_{off} over k_{on}. The affinity constant determined was 68.8 nM. (Dr. Huang from the McNamara lab performed the SPR experiments).

In the study, the pY816 peptide is immobilized onto the sensor chip using biotin/streptavidin affinity coupling, a commonly used technique to tether a ligand onto the sensor chip (*44*). The PLCγ1 tandem SH2 domains protein is then exposed to the sensor chip through the flow channel. SPR measures the refractive index near the sensor surface. The binding of pY816 to PLCγ1 tandem SH2 domains changes the molecular mass of the surface. The change in refractive indices is directly related to the change in the

molecular mass near the sensor chip. The response unit (RU) is extracted and plotted over time, and the curves are fit to obtain the on and off rates of the interactions. Dissociation constant (K_d) is the ratio of the off rate (k_{off}) over the on rate (k_{on}) [*38*]. While ITC is an alternative, it requires larger sample quantity.

2.3 NMR 2D ^{1}H-^{15}N HSQC Titration With the pY816 Peptide

To examine the binding interactions of the nSH2-cSH2 domains bound to the pY816 peptide, we conducted ^{1}H-^{15}N HSQC titration using the pY816 peptide. ^{15}N-labeled protein was prepared from M9 minimal media containing ^{15}N ammonium chloride as the sole nitrogen source. In the 2D ^{1}H-^{15}N HSQC experiment, each amide group yields an NMR signal. The binding of the peptide changes the chemical environment of the amide group, resulting in peak shifts, or chemical shift perturbations.

Increasing concentrations of the peptide were titrated into the PLCγ1 tandem SH2 domain. The resulting chemical shift perturbations as shown in Figure 6 suggest direct interactions of PLCγ1 tandem SH2 domains with pY816. The decrease in the intensity of the cross peaks may be due to sample dilution during the titration.

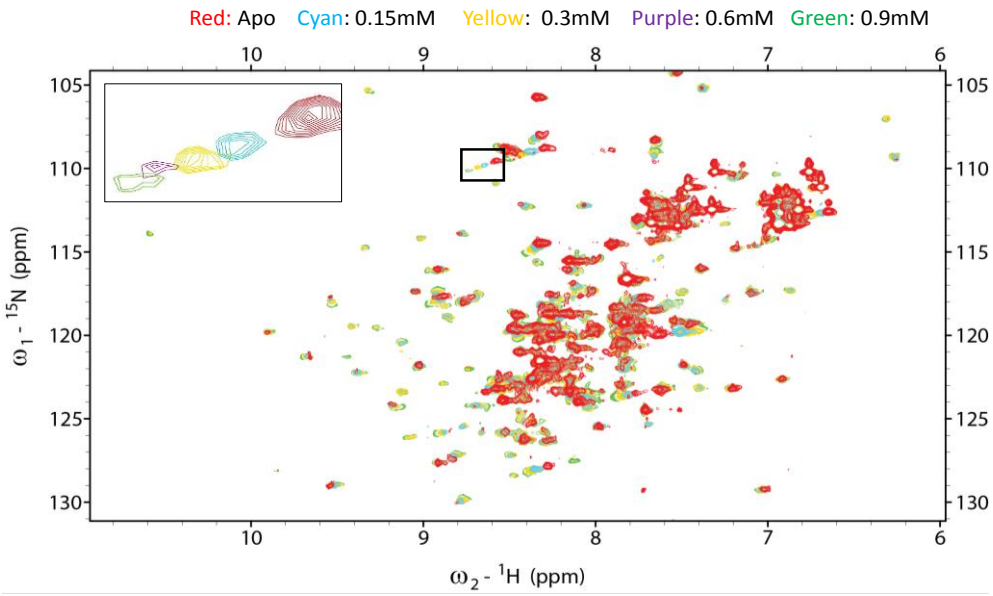

Figure 6. Overlay of NMR 2D ^{1}H-^{15}N HSQC titration spectra of the ^{15}N-labelled nSH2-cSH2 domain in the presence of different concentrations of the pY816 peptide. An increasing concentration of the peptide, from 0.15mM (cyan), 0.3mM (yellow), 0.6mM (purple), to 0.9mM (green) was added to apo-protein (red:0.3mM). Increasing peptide concentrations changes the chemical environment of the apo-protein, resulting in chemical shift perturbations. The inset represents a subset of the overlay spectra.

2.4 Crystallization of the pY816-PLCγ1 Tandem SH2 Domains Complex

To understand the binding mode of the pY816 peptide to PLCγ1 tandem SH2 domains, we attempt to co-crystallize the pY816 peptide with the tandem SH2 domain of PLCγ1. The crystal structure will allow us to gain in-depth insights on the peptide recognition site, and further our understanding on the regulation of PLCγ1 tandem SH2 domains via pY816. Random-matrix screening is a technique commonly used to identify crystallization conditions. Figure 7 shows the initial crystallization hits of the PLCγ1 tandem SH2 domains co-crystallized with the pY816 peptide. Through our initial

crystallization screenings, we have identified a suitable condition for crystal growth. The condition contains 0.17M sodium acetate, 0.085M Tris pH8.5, 25.5% PEG 4000, 15% glycerol. The crystallization conditions will be optimized to obtain a high-resolution structure of the pY816-PLCγ1 tandem SH2 domains complex.

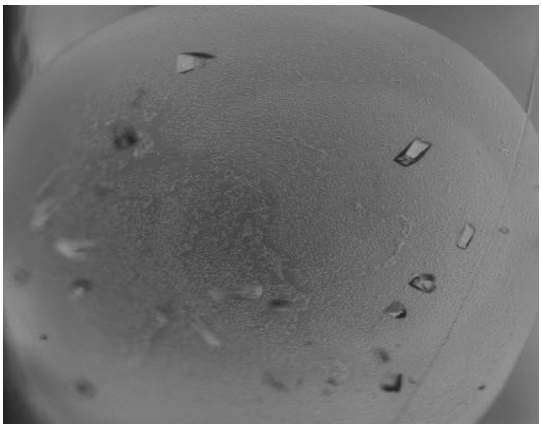

Figure 7. Initial crystallization hits. Initial crystallization hits of PLCγ1 tandem SH2 domains protein generated from random matrix screening.

2.5 Alternative Approach: NMR 2D ^{1}H-^{15}N HSQC Titration of Isolated SH2 Domains with pY816

If our crystallographic efforts are not successful, as an alternative, we propose to co-crystallize individual SH2 domains in complex with the pY816 peptide. Single SH2 domains were generated and expressed as described above. (nSH2: 545Pro to 659 Gln ; cSH2: 660 Thr to 791 Pro). First, we must determine the domain that preferentially forms a complex with the pY816 peptide. We employed 2D ^{1}H-^{15}N HSQC NMR spectroscopy titration experiments on individual SH2 domains using the pY816 peptide to observe chemical shift perturbations. We collected the HSQC spectrum of the nSH2 domain

(0.1mM), shown as red peaks in Figure 8A. Then, an increasing concentration of the pY816 peptide, ranging from 0.05mM (orange), 0.1mM (yellow), 0.2mM (purple), to 0.3mM (green) was titrated into the nSH2 domain. Figure 8A shows the overlay of the spectra obtained from the HSQC titration experiments. Similarly, the peptide was titrated into the cSH2 domain, and the overlay of the spectra is shown in Figure 8B. Intriguingly, preliminary studies show that the chemical shift perturbations of the cSH2 domain is greater than that of the nSH2 domain. This might indicate that the pY816 peptide potentially forms a stronger complex with cSH2 domain.

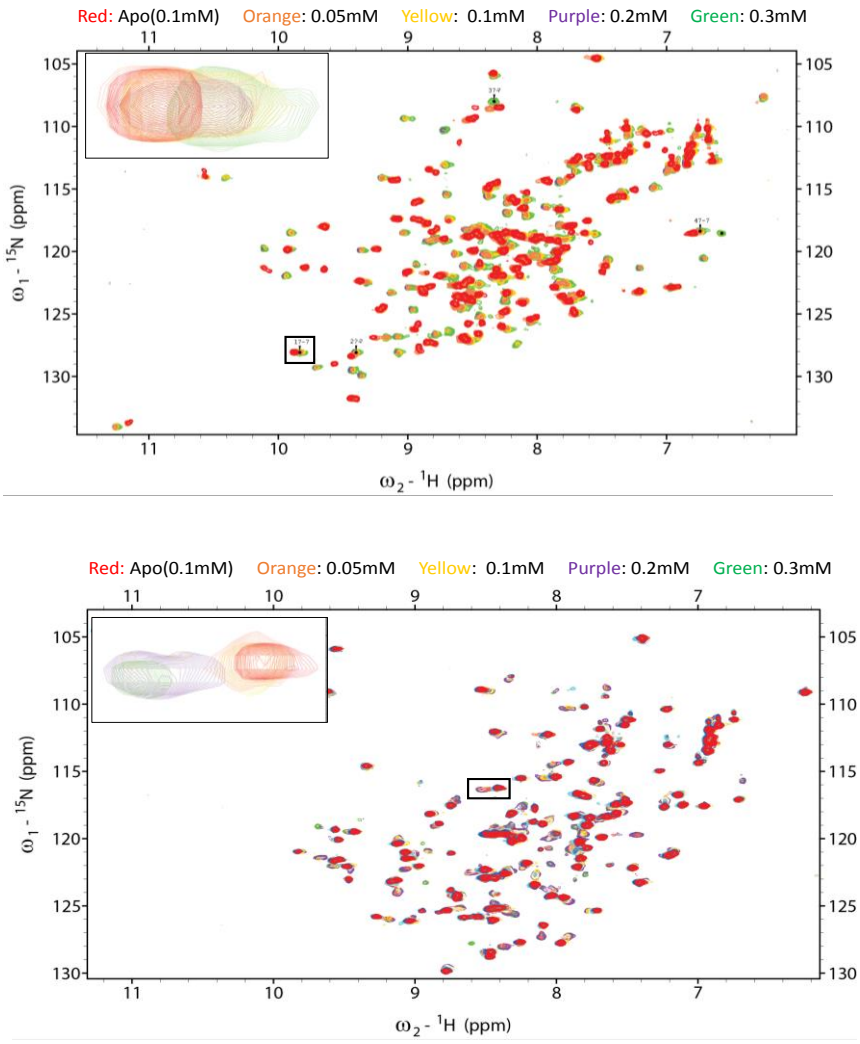

Figure 8: Overlay of NMR 2D ^{1}H-^{15}N HSQC titration spectra of the ^{15}N-labelled nSH2 domain (A) and cSH2 domain (B) against different concentrations of the pY816 peptide. An increasing concentration of the peptide, from 0.05mM (orange), 0.1mM (yellow), 0.2mM (purple), to 0.3mM (green) was added to apo-protein (red:0.1mM). The resulting chemical shift perturbations were shown. Figures A indicates the chemical shift perturbations on the nSH2 domain, whereas figure B shows the perturbations on the cSH2 domain. The greater perturbations on the cSH2 domain might suggest that the cSH2 domain potentially forms a stronger complex with the peptide. The insets represent a subset of the overlay spectra.

Preliminary NMR experiments of the pY816 peptide titrated into nSH2 domain resulted in binding affinity (K_d) of 41.09μM, whereas the binding affinity of the cSH2 domain complexed with the peptide predicted via NMR titration experiment is 54.92μM.

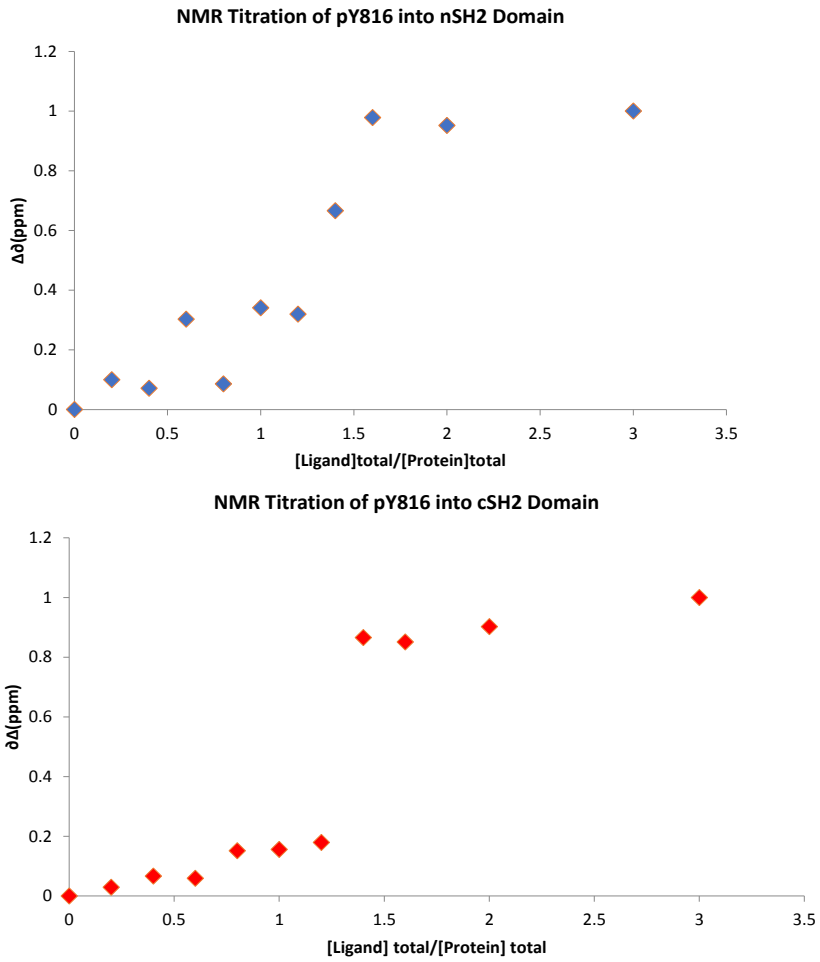

Figure 9: Plot of change in chemical shift of amide resonances versus molar ratio (pY816 concentration/final protein concentration). The upper panel corresponds to the peptide titration into nSH2 domain whereas the bottom panel represents the cSH2 domain, resulting in predicted Kd values of 41.09 and 54.92 μM, respectively.

2.6 Methods and Materials

2.6.1 Optimization of PLCγ1 tandem SH2 domains purification

The PLCγ1 tandem SH2 domain was cloned into a SUMO-fusion pET-based expression vector. The construct contains a 10X Histidine tag for Ni-NTA purification, followed by a SUMO tag as a solubility enhancer, and the protein of interest, the nSH2-cSH2 domains. Protein lysis buffer contains 25mM Tris HCl and 150mM NaCl. Ni-NTA wash buffer contains 25mM Tris HCl, 150mM NaCl, and 40mM imidazole. Protein sample was eluded from the Ni-NTA column in elution buffer containing 25mM Tris, 150mM NaCl, and 300mM imidazole. The SUMO-specific protease, SENP1, was used to cleave the SUMO tag. The reaction was performed at room temperature for 30 minutes. The ratio of protease to protein ratio used was 1:100. SENP1 recognizes the peptide backbone, and no overhang residue is left after cleavage (*40*).

The protein sample was dialyzed in dialysis tubing in buffer containing 25mM Tris HCl, and 150mM NaCl. After overnight dialysis, a second Ni-NTA purification step was performed to remove the SUMO tag, and the flow through fraction was collected. Wash buffer containing 25mM Tris HCl, 150mM NaCl, and 20mM imidazole was used to elute protein sample that remained on the Ni-NTA column. The flow through and wash fractions were collected, pooled, and concentrated to 2mL for a final purification step using size-exclusion chromatography (Superdex200 gel filtration column, in 2mL

fractions), to ensure that the samples are pure and homogenous (Figure 4). The elution buffer contains 10mM HEPES, 150mM NaCl, and 2mM DTT, pH8.0.

2.6.2. NMR titration experiments

The ^{15}N-labelled PLCγ1 tandem SH2 domains protein sample was purified as described above. The protein sample buffer contains 25mM Tris, 150mM NaCl, pH7.5, whereas the pY816 peptide was dissolved in 1xPBS buffer. The stock concentration of the pY816 peptide was 0.615mM. A HSQC spectrum of the apo-protein (0.3mM in 500μL) was collected. An increasing concentration of the peptide, ranges from 0.15mM, 0.3mM, 0.6mM and 0.9mM was added to the same protein sample, and the respective HSQC spectrum at each titration point was collected and overlaid as shown in Figure 6. Table 1 shows the peptide to protein molar ratio, volume of the pY816 peptide added, total sample volume, and final protein concentration at each titration point.

Table 1: 2D ^{1}H-^{15}N HSQC titration experiment of pY816 peptide into PLCγ1 tandem SH2 domains

Peptide to Protein Molar Ratio	Volume of pY816 Peptide Added (μL)	Total Sample Volume (μL)	Final Protein Concentration (mM)
0	0	500.000	0.300
0.5	101.626	601.626	0.249
1.0	203.252	703.252	0.213
2.0	406.504	906.504	0.165
3.0	609.756	1109.756	0.135

The ^{15}N-labelled single domain proteins (nSH2 or cSH2) were purified according to the procedure described above. The starting nSH2 protein sample concentration used was 0.1mM, dissolved in 25mM Tris HCl, 150mM NaCl, 4mM DTT, pH7.5. The pY816 peptide was dissolved in buffer-matched 25mM Tris HCl, 150mM NaCl, 4mM DTT, pH7.5 in a stock concentration of 0.62mM. First, a HSQC spectrum of the apo-protein of 0.1mM (300μL) was collected, in the presence of 10% D_2O. 0.2 molar equivalent of the pY816 peptide was then added to the apo-protein, and the HSQC spectrum was collected. Concentrations of pY816 peptide ranges from 0.4 to 3.0 molar equivalents were subsequently added to the protein sample, and their respective HSQC spectrum was collected. All spectra were processed and overlaid. For optimal visualization purpose, only four titration points were overlaid against the apo-protein, as shown in Figure 8. The

pY816 peptide was added to the same protein sample, and a table of peptide to protein molar ratio, volume of the pY816 peptide added, total sample volume, and final protein concentration at each titration point were shown in Table 2. cSH2 protein sample titration was performed under identical conditions.

Table 2: 2D ^{1}H-^{15}N HSQC titration experiment of pY816 peptide into nSH2 or cSH2 domains

Peptide to Protein Molar Ratio	Volume of pY816 Peptide Added (μL)	Total Sample Volume (μL)	Final Protein Concentration (mM)
0	0	300.0	0.100
0.2	9.756	309.8	0.097
0.4	19.512	319.5	0.094
0.6	29.268	329.3	0.091
0.8	39.024	339.0	0.089
1.0	48.780	348.8	0.086
1.2	58.536	358.5	0.084
1.4	68.293	368.3	0.081
1.6	78.049	378.0	0.079
2.0	97.561	397.5	0.075
3.0	146.341	446.3	0.067

2.6.3 Crystallization of the pY816-PLCγ1 tandem SH2 domains complex

For co-crystallization of the PLCγ1 tandem SH2 domains-pY816 complex, commercially available crystal screens were used to detect optimal conditions for crystal growth. PLCγ1 tandem SH2 domains protein sample was purified in buffer containing 10mM HEPES, 150mM NaCl, 2mM DTT, pH8.0, in concentration of 10.96mg/mL (377μM). The pY816 peptide to protein sample ratio was 1.3 to 1. Initial crystallization generated several crystal hits, yielded from Qiagen screening kit, JCSG IV, well number C3. (Buffer composition: 0.17 M Sodium acetate, 0.085 M Tris pH 8.5, 25.5% PEG 4000, 15% Glycerol) Protein to mother liquor drop ratio used in the crystal screening was 1:1 (1uL of protein sample mixed with 1uL of mother liquor solution. Crystals were seen after 9 days of incubation at 20 ^{0}C. A sample image of protein crystals is shown in Figure 7. Crystals were harvested, protected with cryo-solvent (30% ethelene glycol). Diffraction data were collected at the Advanced Photon Source (APS) at Argonne National Laboratory.

The structure was solved by molecular replacement using the apo-structure of the PLCγ1 tandem SH2 domains as a search model (PDB: 4EY0). Initial crystal hits diffracted to a resolution of 3.2 Å. In these crystals, we were not able to observe the density of the peptide.

As demonstrated in Figure 8, the pY816 peptide might exhibit different affinity towards the nSH2 and the cSH2 domains. If our efforts fail to produce promising crystals for co-crystallization of the nSH2-cSH2 in complex with the pY816 peptide, as an

alternative, we can potentially co-crystallize the pY816 peptide in complex with the nSH2 and cSH2 domain separately as shown by the NMR experiments above.

3. Conclusion

The overall goal of these studies is to understand the molecular details of the engagement of inhibitors with PLCγ1, and study how these inhibitors interact with PLCγ1 to disrupt the TrkB-PLCγ1 interaction.

Our studies have confirmed that the pY816 peptides bind to the PLCγ1 tandem SH2 domain and isolated nSH2 and cSH2 domains. We have also obtained diffraction crystals of the PLCγ1 tandem SH2 domain. A thorough understanding of the interaction of the TrkB-derived pY816 peptide and the PLCγ1 tandem SH2 domain should ultimately facilitate the development of novel therapeutics for the prevention and treatment of TLE.

References

1. Holmes, G., Sirven, J., and Fisher, R.S. (2013) Temporal lobe epilepsy., www.epilepsy.com

2. French, J.A., Williamson, P.D., Thadani, V.M., Darcey, T.M., Mattson, R.H., Spencer, S.S., Spencer, D.D. (1993) Characteristics of medial temporal lobe epilepsy: I. Results of history and physical examination. *Ann. Neurol 34*, 774-780.

3. Paradiso, B., Marconi P., ZucchiniS., Berto E., Binaschi A., Bozac A., Buzzi A., Mazzuferi, M., Magri, E., Navarro, Mora.G., et al. (2009) Localized delivery of fibroblast growth factor-2 and brain-derived neurotropic factor reduces spontaneous seizures in an epilepsy model. *Proc. Natl. Acad. Sci. USA. 106*, 7191-7196.

4. Liu, G., Gu, B., He, X.P., Joshi, R.B., Wackerle, H.D., Rodriguiz, R.M., Wetsel, W.C., McNamara, J.O. (2013) Transient inhibition of TrkB kinase after status epilepticus prevents development of temporal lobe epilepsy. *Neuron 79*, 31-38.

5. Boulle, F., Kenis, G., Cazorla, M., Hamon, M., Steinbusch, H.W.M., Lanfumey, L., Van den Hove, D.L.A. (2012) TrkB inhibition as a therapeutic target for CNS-related disorders. *Progress in Neurobiology 98*, 197-206.

6. Nadler, J.V. (1981) Kianic acid as a tool for the study of temporal lobe epilepsy. *Life Sciences 29*, 2031-2042.

7. Numakawa, T., Suzuki, S., Kumamaru, E., Adachi, N., Richards, M., Kunugi, H. (2010) BDNF function and intracellular signaling in neurons. *Histol Histopathol 2,* 237-58.

8. Minichiello, L. (2009) TrkB signaling pathways in LTP and learning. *Nature Reviews 10,* 850-860.

9. Zhou, S., Shoelson, S.E., Chaudhuri, M., Gish, G. et al. (1993) SH2 domains recognize specific phosphopeptide sequences. *Cell 72*, 767-778.

10. Gu, B., Huang, Y.Z., He, X.P., Joshi, R.B., Jang, W., McNamara, J.O. (2015) A peptide uncoupling BDNF receptor TrkB from phospholipase Cγ1 prevents epilepsy induced by status epilepticus. *Neuron 88*, 484-491.

11. Huang, Z., Marsiglia, W.M., Basu, R.U. et al. (2016) Two FGF Receptor Kinase Molecules Act in Concert to Recruit and Transphosphorylate Phospholipase Cγ. *Molecular Cell 61,* 98-110.

12. Bae, J.H., Lew, E.D., Yuzawa, S., Tome, F., Lax, I., Schlessinger, J. (2009) The Selectivity of Receptor Tyrosine Kinase Signaling Is Controlled by a Secondary SH2 Domain Binding Site *Cell 138*, 514–24.

13. Bunney, T.D., Katan, M. (2011). PLC Regulation: Emerging Pictures for Molecular Mechanisms. *Trends in Biochemical Sciences 36(2),* 88-96.

14. Hajicek, N., Charpentier, T.H., Rush, J.R., Harden, T.K., Sondek, J. (2013) Autoinhibition and Phosphorylation-Induced Activation of Phospholipase C-γ Isozymes. *Biochemistry 52*, 4810-19.

15. Gresset, A., Hicks, S.N., Harden, T.K., Sondek, J. (2010) Mechanism of Phosphorylation-induced Activation of Phospholipase C-γ Isozymes. *JBC 285 (46),* 35836-47.

16. Lemmon, M.A., Schlessinger, J. (2010) Cell Signaling by Receptor Tyrosine Kinases. *Cell 141 (7),* 1117-34.

17. Huang, Y.Z., McNamara, J.O. (2010) Mutual regulation of Src family kinases and the neurotrophin receptor TrkB. *JBC 285* (*11*). 8207-17. doi:10.1074/jbc.M109.091041.

18. Ullrich, A., and Schlessinger, J. (1990) Signal transduction by receptor with tyrosine kinase activity. *Cell 61*, 203-212.

19. Middlemas, D.S., Meisenhelder, J., and Hunter, T. (1993) Identification of TrkB autophosphorylation sites and evidence that phospholipase C-γ1 is a substrate of the TrkB receptor. *JBC 269*. 5458-66.

20. McNamara, J.O, Scharfman, H.E. Temporal Lobe Epilepsy and the BDNF Receptor, TrkB. In: Noebels JL, Avoli M, Rogawski MA, et al., editors. Jasper's Basic Mechanisms of the Epilepsies [Internet]. 4th edition. Bethesda (MD): National Center for Biotechnology Information (US); 2012.

21. Goddard, G.V., McIntyre, D.C., Leech, C.K. (1969) A permanent change in brain function resulting from daily electrical stimulation. *Exp Neurol 25*, 295-330.

22. Doerr, A. (2016) Single-particle cryo-electron microscopy. *Nature Methods 13 (1)*, 23.

23. Reddy, D.S., Kuruba, R. (2013). Experimental models of status epilepticus and neuronal injury for evaluation of therapeutic interventions. *Int. J. Mol. Sci 14*, 18284-18318.

24. Levesque, M., & Avoli, M. (2016). The kianic model of temporal lobe epilepsy. *Neurosci Biobehav Rev 37*,2887-2899.

25. He, X.P., Kotloski, R., Nef, S., Luikart, B.W., Parada, L.F. (2004) Conditional deletion of TrkB but BDNF prevents epileptogenesis in the kindling model. *Neuron 43*, 31-42.

26. Bunney, T.D., Esposito, D., Mas-Droux, C., Lamber, E., Baxendale, RW., Martins, M., Cole, A., Svergun, D., Driscoll, P.C., Katan, M. (2012) Structural and functional integration of the PLCγ interaction domains critical for regulatory mechanisms and signaling deregulation. *Structure 20*, 2062-2075.

27. McNamara, J.O., Huang, Y.Z., and Leonard, A.S. (2006) Molecular signaling mechanisms underlying epileptogenesis. *Sci Signaling 356*, re12.

28. Isackson, P.J., Huntsman, M.M., Murray, K.D., and Gall, C.M. (1991) BDNF mRNA expression is increased in adult rat forebrain after limbic seizures: temporal patterns of induction distinct from NGF. *Neuron 6*, 937-948.

29. He, X.P., Minichiello, L., Klein, R., and McNamara, J.O. (2002) Immunohistochemical evidence of seizure-induced activation of TrkB receptors in the mossy fiber pathway of adult mouse hippocampus. *J. Neuro. Sci*. *22*, 7502-7508.

30. He, X.P., Pan, E., Sciarretta, C., Minichiello, L., and McNamara, J.O. (2010) Disruption of TrkB-mediated PLCγ signaling inhibits limbic epileptogenesis. *J Neurosci 30 (18)*, 6188-6196.

31. Doublié, S. (1997) Preparation of selenomethionyl proteins for phase determination. *Methods in Enzymology 276*, 523-530.

32. Duman, R., Voleti, B. (2012) Signaling pathways underlying the pathophysiology and treatment of depression: novel mechanisms for rapid-acting agents. *Trends in Neurosciences 35(1)*, 47-56.

33. Temporal Lobe: The temporal lobe, which crosses both hemispheres of the brain, helps process sensory input, including pain and auditory stimuli. https://www.spinalcord.com/temporal-lobe.

34. Degorce, F., Card, A., Soh, Sharon., Trinquet, E., Knapik, G.P., Xie, B. (2009) HTRF: A technology tailored for drug discovery- a review of theoretical aspects and recent applications. *Current Chemical Genomics 3*, 22-32.

35. Bertrand, T., Kothe, M., Liu, J., Dupuy, A., Rak, A., Berne, P.F., Davis, S., Gladysheva, T., Valtre, C., Crenne, J.Y., Mathieu, M. (2012) The crystal structures of TrkA and TrkB suggest key regions for achieving selective inhibition. *J. Mol. Biol 423*, 439-453.

36. Cottet, M., Faklaris, O., Maurel, D., Scholler, P., et al. (2012) BRET and time-resolved FRET strategy to study GPCR oligomerization: from cell lines towards native tissues. *Molecular and Structural Endocrinology 3 (92)*.

37. Clow, F., Fraser, J.D., Proft, T. (2008) Immobilization of proteins to biacore sensor chips using *Staphylococcus aureus* sortase A. *Biotechnol Lett 30*, 1603-1607.

38. Kimplea, A.J., Mullera, R.E., Siderovskia, D.P., Willarda, F.S. (2010) A capture coupling method for the covalent immobilization of hexahistidine tagged proteins for surface plasmon resonance. *Methods Mol Biol 627*, 91-100.

39. Riddles, P.W., Blakeley, R.L., Zerner, B. (1983) Reassessment of Ellman's Reagent. *Methods in Enzymology 91*, 49-60.

40. Frey, S., Gorlich, D. (2014) A new set of highly efficient, tag-cleaving proteases for purifying recombinant proteins. *J. Chromatogr A 1337*, 95-105.

41. Bradshaw, J.M., Mitavox, V., Waksman, G. (1999) Investigation of Phosphotyrosine Recognition by the SH2 Domain of the Src Kinase. *J. Mol. Bio 293*, 971-985.

42. Schlessinger, J., and Lemmon, M.A. (2003) SH2 and PTB domains in tyrosine kinase signaling. *Sci. STKE*. *191*, re12.

43. Kobashi, K. (1968) Catalytic oxidation of sulfhdryl groups by o-phenanthroline copper complex. *Biochem. Biophy. Acta. 158*, 239-245.

44. Hutsella, S.Q., Kimpleb, R.J., Siderovskic, D.P., Willardc, F.S., Kimplec, A.J. (2010) High affinity immobilization of proteins using biotin- and GST- based coupling strategies. *Methods Mol. Biol. 627*, 75-90.

45. Grassucci, R.A., Taylor, D.J., & Frank, J. (2007) Preparation of macromolecular complexes for cryo-electron microscopy. *Nature Protocols. 2(12),* 3239-3246.